THE JOURNAL OF CHEMICAL PHYSICS **127**, 144313 (2007)

Geometries and stabilities of Ag-doped Si_n ($n=1-13$) clusters: A first-principles study

Feng-Chuan Chuang, Yun-Yi Hsieh, Chih-Chiang Hsu, and Marvin A. Albao
Department of Physics, National Sun Yat-Sen University, Kaohsiung 804, Taiwan

(Received 20 June 2007; accepted 31 July 2007; published online 12 October 2007)

The structures of $AgSi_n$ ($n=1-13$) clusters are investigated using first-principles calculations. Our studies suggest that $AgSi_n$ clusters with $n=7$ and 10 are relatively stable isomers and that these clusters prefer to be exohedral rather than endohedral. Moreover, doping leaves the inner core structure of the clusters largely intact. Additionally, the plot of fragmentation energies as a function of silicon atoms shows that the $AgSi_n$ are favored to dissociate into one Ag atom and Si_n clusters. Alternative pathways exist for $n>7$ (except $n=11$) in which the Ag–Si cluster dissociates into a stable Si_7 and a smaller fragment $AgSi_{n-7}$. The $AgSi_{11}$ cluster dissociates into a stable Si_{10} and a small fragment AgSi. Lastly, our analysis indicates that doping of Ag atom significantly decreases the gaps between the highest occupied molecular orbital and the lowest unoccupied molecular orbital for $n>7$. © *2007 American Institute of Physics*. [DOI: 10.1063/1.2775447]

I. INTRODUCTION

The metal-doped silicon clusters or cages have been the subject of extensive theoretical and experimental investigations.[1–3] Specifically, research in pure silicon and metal-doped silicon clusters is wide ranging and is currently a staple in certain areas of chemistry and physics. Much of the excitement in this field derives from the fact that the properties of these clusters are markedly different from those of bulk materials, thus generating enormous interest among theoretical materials scientists. Additionally, potential applications of materials with novel properties based on metal-doped silicon clusters and metal-doped fullerenes are of significant importance to materials engineers working in the semiconductor industry. To this end, numerous experimental and theoretical studies[3–5] have been devoted to the determination of equilibrium geometries, electronic and bonding structures, as well as structural transition of different sizes of pure silicon clusters and metal-doped silicon clusters.

Despite the general interest in metal-doped silicon cluster, the number of studies devoted to group IB (Cu, Ag, and Au) metals is surprisingly limited compared to similar systems involving metal-doped silicon clusters.[2,3] Recently, Jaeger *et al.* were able to successfully demonstrate some of the desired metal-silicon clusters for silver and copper.[6] Although copper-silicon clusters had already been reproduced prior to this pioneering work, production of silver had remained elusive up until that point. In that work, they reported that the mass spectrum of silver-silicon cluster was similar to that for copper-silicon. In addition, the most abundant silver-silicon product turned out to be $AgSi_7$ and $AgSi_{10}$. These two cluster sizes were prominent and no other mixed cluster size was produced with high enough concentration for its photodissociation to be studied properly. Their photodissociation data showed that the most abundant fragment ions are Si_7^+ and Si_{10}^+ for $AgSi_7^+$ and $AgSi_{10}^+$, respectively. From these findings, we can deduce that the structures of these clusters should have an external metal and that the Ag–Si bonding is weaker on average than Si–Si bonding. Unfortunately, except for a couple of articles on $AgSi_n$ ($2<n<13$) species,[7,8] virtually no other studies specifically address theoretical structures or bonding energetics for the Ag–Si clusters. Here we point out that a recent comparative study[8] by Gueorguiev *et al.* used the caged structures for Ag-doped silicon clusters.[2] Their research indicated that not all of these metals share the same structures and exhibit the same stable size. The structures considered by Gueorguiev *et al.* for $AgSi_7$ and $AgSi_{10}$ are endohedral.[8] In contrast, these same structures are found to be exohedral[6] by Jaeger *et al.* In view of the seeming lack of agreement between these studies, it is still highly desirable to perform an extensive and perhaps conclusive study on Ag-doped Si clusters.

In this paper, a search for candidate low energy structures is performed for each size of $AgSi_n$ clusters. Our calculations showed that the previous proposed endohedral metal structures for $AgSi_n$ ($n=9-12$) are not the lowest energy models. We report on the details of these findings in Sec. III. The rest of the paper is organized as follows: In Sec. II, we describe our computational methods. The bulk of our work is presented in Sec. III, along with an analysis of the stability of these clusters. Finally, we summarized our findings in Sec. IV.

II. COMPUTATIONAL DETAILS

The calculations for both Ag-doped silicon clusters and pure silicon clusters were done within the generalized gradient approximation[9] to spin polarized density functional theory[10] using projector-augmented-wave potentials,[11] as implemented in Vienna *ab initio* simulation package (VASP).[12] The kinetic energy cutoff is set to 249.8 eV (18.36 Ry). The structural optimization was done with the conjugate gradient algorithm and without symmetry until the forces on the atoms are less than 0.001 eV/Å. For the $AgSi_n$ and Si_n clusters, the length of the supercell is set to 15 Å. In order to optimize certain proposed models, a quasi-Newtonian algorithm was used to relax models to their local minima. To check the validity of our methodology, we first performed first-principles calculations on pure silicon clusters Si$_n$ (n=2–13), whose results are well known from previous studies by Liu *et al.*[13] and Lu *et al.*[14]

To determine whether Ag atoms are endohedral or exohedral, we generated numerous initial structures for each Ag-doped silicon cluster size and proceeded to perform structural optimizations using first-principles total energy calculations. A natural starting point is to take the structures of ReSi$_n$,[15] TaSi$_n$,[16] and WSi$_n$ (Ref. 2) clusters as well as several other known structures from the literature[8,17–21] as candidates for the lowest energy structures of Ag-doped Si clusters. We are also able to generate additional structures using two other general approaches. One such approach entails replacing one Si atom in a pure Si$_{n+1}$ cluster with a Ag atom to create a new structure for AgSi$_n$. The second approach involves capping a pure Si$_n$ cluster with Ag at selected positions to create a AgSi$_n$ cluster. Overall, over 50 structures for each AgSi$_n$ (n=8–13) cluster size are optimized in this way. However, it should be pointed out that the present approach may not be appropriate in cases where a silicon cluster is doped with two or more additional metal atoms. In this case, structural optimizations require more sophisticated approaches such as genetic algorithm.[22]

III. RESULTS AND DISCUSSIONS

A. Structures of AgSi$_n$ (n=1–13)

In this section, the key results of our search for the lowest energy structures of AgSi$_n$ (n=1–13) clusters are presented. Figures 1–7 illustrate selected low energy isomers for each size.

Starting with the smallest cluster AgSi, our calculations reveal that the bond lengths of Si dimer, Ag dimer, and AgSi dimer are 2.28, 2.56, and 2.36 Å, respectively. The bond length of 2.36 Å for AgSi is comparable to the experimental value of 2.40 Å and not very far from the theoretical result of 2.39 Å at complete active space perturbation theory of second order level which takes into account relativistic effective core potentials.[23,24]

For AgSi$_2$, the optimized geometry shown in Fig. 1(a) is an isosceles triangle in which the bond lengths are 2.48 Å for Ag–Si and 2.17 Å for Si–Si. For the bond angles, we obtained the values of 51.8° for Si–Ag–Si and 64° for Ag–Si–Si. We also determined that the next lowest geometry shown in Fig. 1(b) is obtained by capping one end of the Si dimer by a Ag atom, resulting in a linear structure. For the third isomer shown in Fig. 1(c), the Si–Ag–Si bond angle is 127.5°, with the two Si–Ag bonds differing only slightly in length (2.355 vs 2.366 Å).

For the AgSi$_3$ cluster, our data indicate that a planar rhombus is favored over a pyramid by 100 meV/atom as shown in Figs. 1(e) and 1(h). One can regard AgSi$_3$ [Fig. 1(a)] as Si trimer capped by a Ag atom.

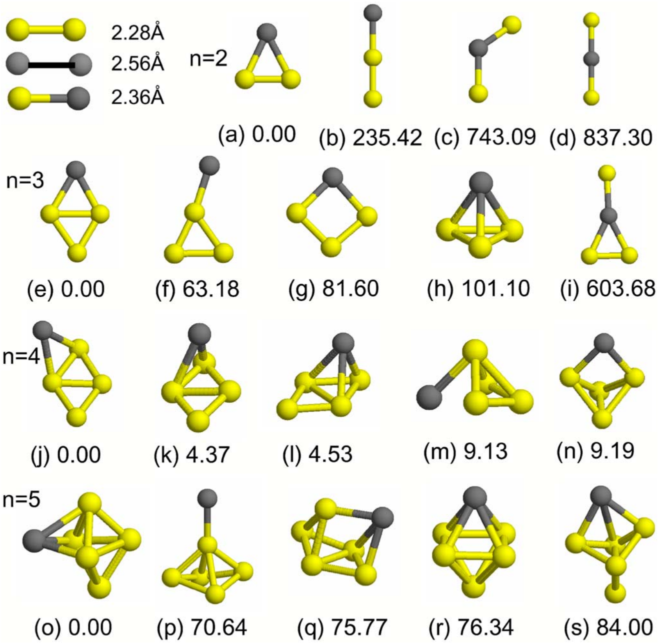

FIG. 1. (Color online) (a) Si dimers, Ag dimers, and Ag silicides, along with their bond lengths. The lowest energy isomers of neutral AgSi$_2$ to AgSi$_5$ are shown. The numbers under the structures are relative energies per atom (in meV/atom) with respect to that of the lowest energy isomer of the same size. The Si atoms and Ag atoms are shown in yellow (light gray) and gray (dark gray), respectively.

Moving on to the next bigger cluster, we found that the most stable structure for AgSi$_4$ is one in which the edge of a D_{2h} rhombus Si$_4$ is capped by a Ag atom, as shown in Fig. 1(j). For AgSi$_5$, however, the most stable isomer appears to be a Ag atom adsorbed on a bipyramid (hexahedron) of Si$_5$, as illustrated in Fig. 1(o). Figure 1(p) is one silver atom adsorbed on top of a slightly distorted square pyramid of Si$_5$. Finally, another isomer of AgSi$_5$ of note is an octahedron with Ag on one corner (square bipyramid), as shown in Fig. 1(r).

Likewise, for AgSi$_6$, one can create a stable isomer by

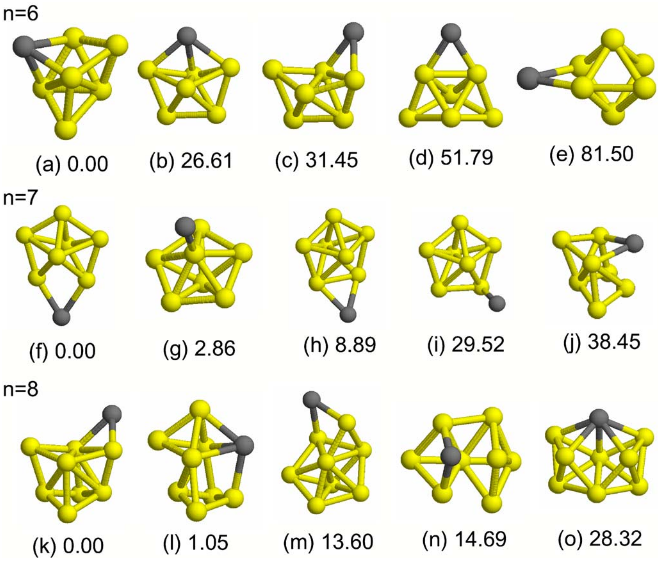

FIG. 2. (Color online) The lowest energy isomers of neutral AgSi$_6$, AgSi$_7$, and AgSi$_8$. The numbers under the structures are relative energies per atom (in meV/atom) with respect to that of the lowest energy isomer of the same size. The Si atoms and Ag atoms are shown in yellow (light gray) and gray (dark gray), respectively.

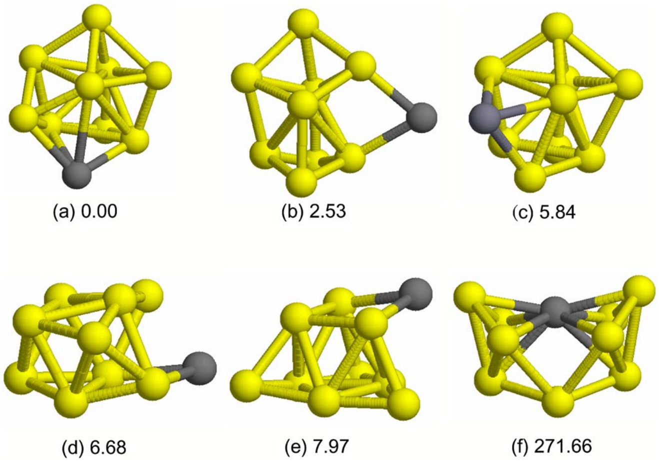
(a) 0.00 (b) 2.53 (c) 5.84

(d) 6.68 (e) 7.97 (f) 271.66

FIG. 3. (Color online) The lowest energy isomers of neutral $AgSi_9$. The numbers under the structures are relative energies per atom (in meV/atom) with respect to that of the lowest energy isomer of the same size. The Si atoms and Ag atoms are shown in yellow (light gray) and gray (dark gray), respectively.

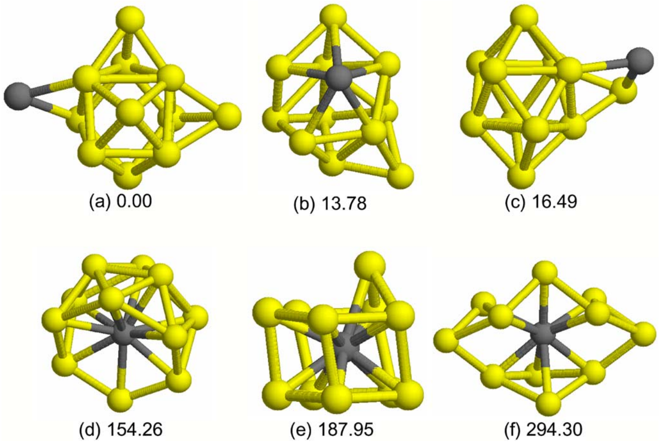
(a) 0.00 (b) 13.78 (c) 16.49

(d) 154.26 (e) 187.95 (f) 294.30

FIG. 5. (Color online) The lowest energy isomers of neutral $AgSi_{11}$. The numbers under the structures are relative energies per atom (in meV/atom) with respect to that of the lowest energy isomer of the same size. The Si atoms and Ag atoms are shown in yellow (light gray) and gray (dark gray), respectively.

taking the most stable isomer of $AgSi_5$ and capping it with an additional Si, as shown in Fig. 2(a), that is, one Ag and one Si atom capping a bipyramid (hexahedron) of Si_5. Another low energy isomer can be generated by substituting one Si in a pentagonal bipyramid of Si_7 with a Ag atom, as shown in Fig. 2(b). We also included other low energy isomers for comparison.

The low energy isomers for $AgSi_7$ are plotted in Figs. 2(f)–2(j). Among the possible $AgSi_7$ structures, the one with the lowest energy [Fig. 2(f)] appears to be a pentagonal bipyramid of Si_7 in which a Ag atom is attached to the side and coplanar with the plane defined by the pentagon.

So far, a trend has emerged in which the most stable isomers for a particular cluster size appear to have been generated by capping a low energy Si_n isomer with a Ag atom. This pattern continues for certain cluster sizes, though an approach in which substituting a Si atom with a Ag atom and moving the former to a different position may also become important.

A case in point is $AgSi_8$ which is illustrated in Fig. 2(k). Here, a top Si atom of the lowest energy isomer of Si_9 (bicapped pentagonal bipyramid) is removed and is substituted for by a Ag atom which is then moved away from this initial position. Figure 2(l) is essentially the lowest energy isomer of Si_9 where one of the capping Si atoms is replaced by a Ag atom. Figure 2(m) is one Ag atom capping the lowest energy isomer of Si_8 (Ref. 13).

For $AgSi_9$, the low energy isomers are structurally related to Si_9. To understand the lowest energy structure for this size, we start with the isomer shown in Fig. 3(c) in which one Ag is adsorbed on the Si_9. Next, we switch the position of the Ag atom with one of the Si atoms, as shown in Fig. 3(a). Other low energy isomers for this size include one wherein a Ag atom is adsorbed on the lowest energy

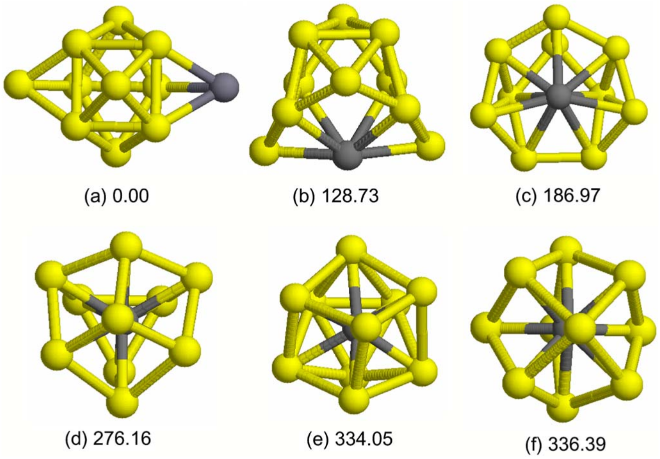
(a) 0.00 (b) 128.73 (c) 186.97

(d) 276.16 (e) 334.05 (f) 336.39

FIG. 4. (Color online) The lowest energy isomers of neutral $AgSi_{10}$. (a) One Ag and one Si atom cap the tricapped trigonal prism (TTP) of Si_9. [(b) and (c)] Open structures. (d) Tetracapped trigonal prism. (e) Capped pentagonal-rhombus structure (three fold). (f) Bicapped square antiprism. The numbers under the structures are relative energies per atom (in meV/atom) with respect to that of the lowest energy isomer of the same size. The Si atoms and Ag atoms are shown in yellow (light gray) and gray (dark gray), respectively.

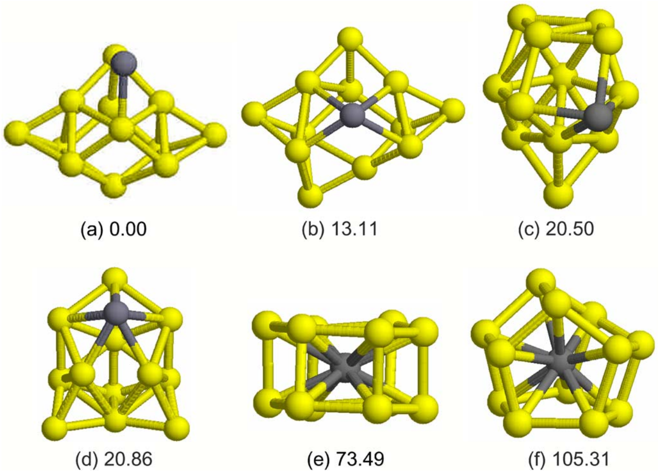
(a) 0.00 (b) 13.11 (c) 20.50

(d) 20.86 (e) 73.49 (f) 105.31

FIG. 6. (Color online) The lowest energy isomers of neutral $AgSi_{12}$. The numbers under the structures are relative energies per atom (in meV/atom) with respect to that of the lowest energy isomer of the same size. The Si atoms and Ag atoms are shown in yellow (light gray) and gray (dark gray), respectively.

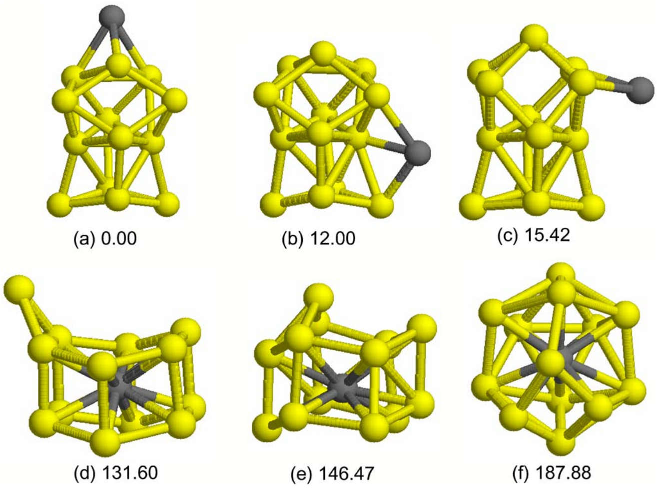

FIG. 7. (Color online) The lowest energy isomers of neutral $AgSi_{13}$. The numbers under the structures are relative energies per atom (in meV/atom) with respect to that of the lowest energy isomer of the same size. The Si atoms and Ag atoms are shown in yellow (light gray) and gray (dark gray), respectively.

isomer of Si_9 [see Fig. 3(b)] and another in which a Ag atom is adsorbed on a tricapped trigonal prism (TTP) unit of Si_9 [see Fig. 3(d)]. Figure 3(e) shows a tetrahedral pyramid of Si_9, but with the top atom displaced, leaving it slightly protruding on the side. For comparison with other proposed structures, we included a caged isomer by Khanna *et al.* for $FeSi_9$ [see Fig. 3(f)] whose energy is relatively higher than that of the lowest energy isomer by 271.66 meV/atom.[19]

Doping of Ag in Si_{10} is generally favored outside, as shown in Fig. 4(a). These structures tend to retain the TTP of Si_9 having one silicon atom and one silver atom capping the TTP. We also examined the other structural models of metal-doped Si_{10},[8,18,19] as shown in Fig. 4. Figures 4(b) and 4(c) are open structures. Figures 4(d)–4(f) are tetracapped trigonal prism, capped pentagonal-rhombus structure (three fold), and bicapped square antiprism. From these, we are able to conclude that the center-site structures are unfavorable for $AgSi_{10}$ and are relatively high in energy compared to those in the adsorption and substitutional structures.

The six low energy isomers for $AgSi_{11}$ are plotted in Fig. 5. The lowest energy isomer as shown in Fig. 5(a) is identified as one silicon atom capping a $AgSi_{10}$ in Fig. 4(a). Similar structures can be generated using the same procedure of capping by Ag atom, but with the latter atom sampling different positions, resulting in slightly higher energies. They are illustrated in Fig. 5(c). A structure is created by dislodging a Si atom and replacing with Ag, in the process shown in Fig. 5(b). We also evaluated three caged isomers shown in Figs. 5(d)–5(f) and found that their energies are relatively high.[19,20]

Likewise, we identified six low energy isomers for $AgSi_{12}$, shown in Fig. 6. It turns out that the lowest energy isomer can be obtained by adsorbing a Ag atom on the lowest energy isomer for Si_{12} obtained from Ref. 13. Additionally, one can generate two isomers shown in Figs. 6(b) and 6(c) by replacing a Si atom with a Ag atom, with the former moved to a different position (with respect to Si_{12}) and thereby displacing one Si atom. Figure 6(d) is the Ag atom embedded on the cluster surface with a high coordination number of 5. Figures 6(e) and 6(f) are the known Si_{12} caged clusters formed by encapsulation of a metal atom.[2]

Finally, the six low energy isomers for $AgSi_{13}$ are displayed in Fig. 7. Among them is the lowest energy isomer shown in Fig. 7(a) and is created merely by the generic method of capping Si_{13} with a Ag atom. Similar structures can be generated using the same capping mechanism, but with different positions of the Ag atom, resulting in slightly higher energies. They are illustrated in Figs. 7(b) and 7(c). We also evaluated three caged isomers shown in Figs. 7(d)–7(f), and found that their energies are relatively high. They are created by adding a Si atom on the caged $AgSi_{12}$ in the process shown in Figs. 7(d)–7(f).[20]

Overall, we found that for sizes $n=1-13$, the $AgSi_n$ clusters tend to be exohedral silver. Our studies suggest that the silver atom generally prefers to cap a pure silicon rather than substituting a silicon atom in the cluster. This specific structural feature is in contrast with that of group VIB transition metals (W and Cr) in which endohedral atoms are the preferred structure. Furthermore, for the relatively stable pure Si clusters ($n=7$ and 10), doping leaves the inner core structure mostly intact. However, for the relatively unstable pure Si clusters ($n=5,6,8,9$), substitution increasingly becomes as important as capping and may even dominate in certain cases, causing structural changes in the clusters. Additionally, for $n>10$, we were able to confirm that the TTP unit of Si_9 is the predominant structural feature for $AgSi_n$ and Si_n.

B. Relative stability of $AgSi_n$

A central concept in any stability analysis of clusters is the binding energy per atom, which we define here as

$$E_b(AgSi_n) = -[E(AgSi_n) - E(Ag) - nE(Si)]/(n+1) \tag{1}$$

and

$$E_b(Si_n) = -[E(Si_n) - nE(Si)]/n, \tag{2}$$

where $E(Ag)$ and $E(Si)$ are the single atom energies for Ag and Si and $E(AgSi_n)$ and $E(Si_n)$ are the total energies for $AgSi_n$ and Si_n. The binding energies (per atom) for Ag-doped Si clusters and pure Si clusters as a function of cluster size are plotted in Fig. 8(a). Notice that two curves exhibit the same trend for $n>7$. It also shows that for pure silicon clusters, those with size $n=7$ and 10 are stable, whereas for Ag-doped Si clusters only $n=10$ appears to be stable. We further note that the binding energies of Ag-doped Si clusters are generally smaller than their pure Si cluster counterparts. This implies that doping *per se* does not always enhance cluster stability as we have seen in Ag-doped silicon clusters.

The relative stability of the clusters can also be classified according to the second difference in binding energy per atom defined by

$$\Delta^2E(AgSi_n) = -2E_b(AgSi_n) + E_b(AgSi_{n+1}) + E_b(AgSi_{n-1}) \tag{3}$$

and

$$\Delta^2E(Si_n) = -2E_b(Si_n) + E_b(Si_{n+1}) + E_b(Si_{n-1}). \tag{4}$$

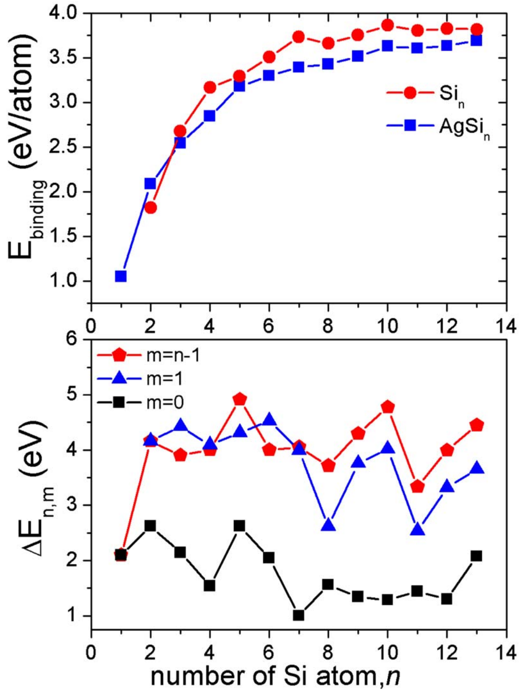

FIG. 8. (Color online) (a) Binding energy vs size of the cluster. (b) Fragmentation energy $[\Delta E_{n,m}=E(\mathrm{AgSi}_m)+E(\mathrm{Si}_{n-m})-E(\mathrm{AgSi}_n)]$ vs size of the cluster. The most dominant channel ($m=0$) for the fragmentation energy is the evaporation of a silver atom from the cluster.

In Fig. 9(a), we plotted $\Delta^2 E(n)$ as a function of cluster size. Stability analysis based on this plot suggests that for pure Si_n, clusters of size 7 and 10 are relatively stable. For $AgSi_n$, the same analysis points toward stability of size $n=5,7$, in addition to $n=10$ which we already identified earlier based on binding energy curve analysis. The sharp decrease in $\Delta^2 E(n)$ due to Ag doping is prominent for Si_7. For small $AgSi_n$ ($n<5$), we can see a trend reversal in the sense that for pure Si clusters $\Delta^2 E(n)$ is generally higher than in their Ag-doped counterparts. Based on this analysis, it is clear that our results agree with the mass spectrum data obtained by Jaeger *et al.*[6] in which they found that most abundant silver-silicon clusters are $AgSi_7^+$ and $AgSi_{10}^+$.

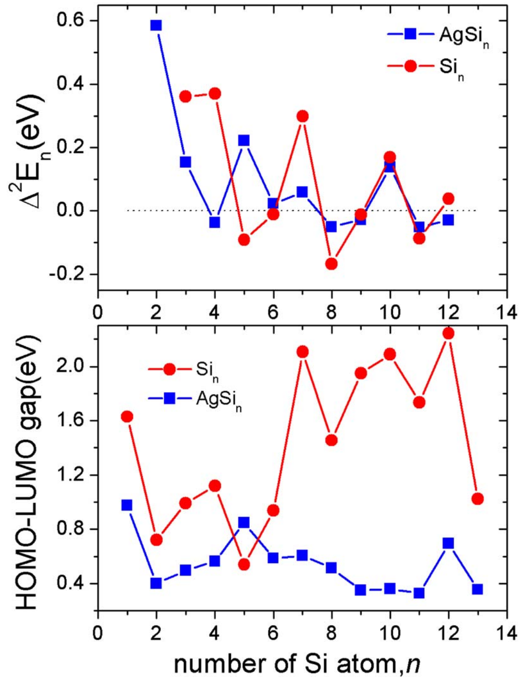

FIG. 9. (Color online) (a) The second difference in binding energy and (b) the HOMO-LUMO gap as a function of the number of atoms in the clusters.

Similarly, studies of fragmentation pathways and dissociation energies also provide useful information for understanding the stability of the clusters. It is well known that clusters which frequently appear in the fragmentation products are likely to be relatively stable. Since fragment analysis for pure silicon clusters has already been done by Liu *et al.*[13] and Shvartsburg *et al.*,[25] we will not present our own results here. Instead, we will focus on the Ag-doped Si clusters and compare our results to that obtained experimentally by Jaeger *et al.*[6]

The energy needed to dissociate a neutral $AgSi_n$ cluster into $AgSi_m$ and Si_{n-m} clusters is given by

$$\Delta E_{n,m}=E(\mathrm{AgSi}_m)+E(\mathrm{Si}_{n-m})-E(\mathrm{AgSi}_n), \qquad (5)$$

where $E(\mathrm{AgSi}_m)$ is the total energy of the cluster with m silicon atoms ($0\leqslant m\leqslant n-1$). Setting $m=0$ yields the energy needed to dissociate a neutral $AgSi_n$ cluster into one silver atom and a Si_n cluster, whereas setting $m=n-1$ gives the energy needed to dissociate a silicon atom from the $AgSi_n$ clusters. In the $m=0$ case, $E(\mathrm{Si}_n)$ corresponds to the energy of a pure Si_n cluster and $E(\mathrm{Ag})$ is the energy of a Ag atom. We evaluated the fragmentation energies of the neutral clusters for all possible pathways and provided plots for key pathways in Fig. 8(b). We found that the primary pathway (most dominant channel) is the evaporation of a silver atom from a cluster. This result is in agreement with the photodissociation data of $AgSi_7^+$ and $AgSi_{10}^+$ obtained by Jaeger *et al.*[6] We also found a secondary pathway for $n>7$ (except $n=11$) in which the Ag–Si cluster dissociates into Si_7 and a smaller fragment $AgSi_{n-7}$. The $AgSi_{11}$ cluster dissociates into Si_{10} and a small fragment AgSi, noting that $n=10$ is also stable.

Therefore, dissociation energies together with the previous structural analysis provide compelling evidence that Ag-doped Si_7 and Si_{10} clusters prefer to be exohedral rather than endohedral.

C. Electronic properties of $AgSi_n$

The HOMO-LUMO gap (the difference between the highest occupied molecular orbital and the lowest unoccupied molecular orbital) is the prototypical electronic property and is an invaluable tool in cluster stability analysis. In this work, the HOMO-LUMO gaps of the lowest energy isomers of each cluster size are evaluated using spin-polarized density functional theory calculations. The data in Fig. 9(b) show that the $AgSi_n$ clusters with $n=1$, 5, and 12 exhibit relatively wider HOMO-LUMO gaps. Figure 9(b) also shows that the doping Ag atom significantly decreases the HOMO-LUMO gaps for $n>7$. For pure Si clusters, these results strongly suggest a correlation between the HOMO-LUMO gaps and the energetic stability, whereas for the Ag-doped Si clusters, our data are inconclusive.

IV. CONCLUSION

In summary, we have calculated the energetics of neutral $AgSi_n$ clusters ($n=1-13$) corresponding to their equilibrium geometries. Our results indicate that Ag atom prefers to cap the Si clusters rather than be embedded inside Si clusters. Specifically, $AgSi_7$ and $AgSi_{10}$ are found to be two relatively stable clusters, in agreement with experimental observations.[6] In addition, for these clusters, doping leaves the inner core structure of the clusters largely intact. In contrast, the same study reveals that especially for relatively unstable clusters, substitution may compete with capping and may cause structural changes in the inner structure. Additionally, fragmentation analysis reveals that the primary pathway is through evaporation of a silver atom from a Ag-doped clusters, which is also consistent with experimental data.[6] Our data have also uncovered a secondary pathway for $n>7$ (except $n=11$) in which the Ag–Si cluster dissociates into Si_7 and a smaller fragment $AgSi_{n-7}$. The $AgSi_{11}$ cluster dissociates into a stable Si_{10} and a small fragment AgSi.

ACKNOWLEDGMENTS

This work was supported by the NCTS and the National Science Council of Taiwan under Grant No. NSC95-2112-M110-022. The authors are grateful to the National Center for High-performance Computing in Taiwan for computer time and facilities.

[1] S. M. Beck, J. Chem. Phys. **87**, 4233 (1987).
[2] H. Hiura, T. Miyazaki, and T. Kanayama, Phys. Rev. Lett. **86**, 1733 (2001).
[3] V. Kumar and Y. Kawazoe, Phys. Rev. Lett. **87**, 045503 (2001).
[4] A. K. Singh, T. M. Briere, V. Kumar, and Y. Kawazoe, Phys. Rev. Lett. **91**, 146802 (2003); H. Kawamura, V. Kumar, and Y. Kawazoe, Phys. Rev. B **70**, 245433 (2004); **71**, 075423 (2005).
[5] V. Kumar, A. K. Singh, and Y. Kawazoe, Phys. Rev. B **74**, 125411 (2006).
[6] J. B. Jaeger, T. D. Jaeger, and M. A. Duncan, J. Phys. Chem. A **110**, 9310 (2006).
[7] P.-F. Zhang, J.-G. Han, and Q.-R. Pu, THEOCHEM **634**, 25 (2003).
[8] G. K. Gueorguiev, J. M. Pacheco, S. Stafstrom, and L. Hultman, Thin Solid Films **515**, 1192 (2006); G. K. Gueorguie and J. M. Pacheco, J. Chem. Phys. **119**, 10313 (2003).
[9] J. P. Perdew, K. Burke, and M. Ernzerhof, Phys. Rev. Lett. **77**, 3865 (1996).
[10] P. Hohenberg and W. Kohn, Phys. Rev. **136**, B864 (1964); W. Kohn and L. J. Sham, Phys. Rev. **140**, A1135 (1965).
[11] G. Kresse and D. Joubert, Phys. Rev. B **59**, 1758 (1999).
[12] G. Kresse and J. Hafner, Phys. Rev. B **47**, 558 (1993); G. Kresse and J. Furthmuller, *ibid.* **54**, 11169 (1996).
[13] B. Liu, Z.-Y. Lu, B. Pan, C.-Z. Wang, K.-M. Ho, A. A. Shvartsburg, and M. F. Jarrold, J. Chem. Phys. **109**, 9401 (1998).
[14] Z.-Yi Lu, C.-Z. Wang, and K.-M. Ho, Phys. Rev. B **61**, 2329 (2005).
[15] J.-G. Han, Z.-Y. Ren, and B.-Z. Lu, J. Phys. Chem. A **108**, 5100 (2004).
[16] P. Huo, Z.-Y. Ren, F. Wang, J. Bian, J.-G. Han, and G.-H. Wang, J. Chem. Phys. **121**, 12265 (2004).
[17] J. Wang and J.-G. Han, J. Chem. Phys. **123**, 064306 (2005).
[18] V. Kumar, A. K. Singh, and Y. Kawazoe, Nano Lett. **4**, 677 (2004).
[19] S. N. Khanna, B. K. Rao, P. Jena, and S. K. Nayak, Chem. Phys. Lett. **373**, 433 (2003).
[20] S. N. Khanna, B. K. Rao, and P. Jena, Phys. Rev. Lett. **89**, 016803 (2002).
[21] N. Uchida, T. Miyazaki, and T. Kanayama, Phys. Rev. B **74**, 205427 (2006).
[22] D. M. Deaven and K. M. Ho, Phys. Rev. Lett. **75**, 288 (1995).
[23] P. Turski, Chem. Phys. Lett. **325**, 115 (1999).
[24] J. J. Scherer, J. B. Paul, C. P. Collier, and R. J. Saykally, J. Chem. Phys. **103**, 113 (1995).
[25] A. A. Shvartsburg, M. F. Jarrold, B. Liu, Z.-Y. Lu, C.-Z. Wang, and K.-M. Ho, Phys. Rev. Lett. **81**, 4616 (1999).